Theory of Ion Boundary Layers

RONALD A. JOHNSON* AND P. C. T. DE BOER†
Cornell University, Ithaca, New York

Theories are presented for the electric boundary layers that form on flat-plate and cylindrical probes aligned parallel with a high speed flow, when the probe potential is large and negative. Both slightly ionized continuum flows and collisionless plasmas are considered. In the former case, the probe potential is supposed sufficiently large to make the electric boundary layer thick compared with the viscous boundary layer. The corrections arising from the presence of the viscous boundary layer are calculated. The cases considered are solved either by an integral method, or by a quasi-one-dimensional method. The results obtained can be used to determine the freestream ion density from the current measured experimentally. A comparison is made between theory and some available experimental data.

I. Introduction

In recent years, considerable attention has been focused on the theory of electric probes which can be used for measuring the number density of charged particles in a plasma. Although earlier work was mainly restricted to the case where the plasma is at rest,[1] there presently is much interest in flowing plasmas. Various investigators have described probe measurements in high-speed, low-density flows where the sheath or electric boundary layer is assumed free molecular.[2-7] Of particular interest in connection with the present study is the work of Ref. 6, which established that when the ratio of the radius r_p of a cylindrical probe aligned with the flow, to the Debye length h_e is greater than 3, the experimental ion saturation current is larger than that predicted by theories neglecting the presence of the flow. The theory including flow effects for this case is given in Sec. V of the present paper. A comparison with the experimental results of Ref. 6 is given in Sec. VI.

A number of theoretical treatments has been given for electric probes immersed in flowing continuum plasmas. Most of these studies[8-17] were limited to cases where the viscous boundary layer is much thicker than the ion sheath. This allows neglecting convection within the sheath. The resulting ion flow in the sheath can be treated as one-dimensional, which is crucial in solving the sheath equations.[13] On the other hand, at low densities of the charged particles and at large probe potential, the sheath becomes very thick, and can be made to fill a hollow probe. The probe then serves as a total collector of all charged particles convected into its entrance area.[18,19] If the density of the charged particles is increased, the sheath thickness decreases. There may arise a situation where the sheath can no longer fill a hollow probe of practical size, but still is thick compared with the viscous boundary layer. An approximate theory for such a sheath was given in Ref. 20. Recently, the result of this theory was shown to be the lowest order result of a strict treatment of the basic equations, in which the asymptotic limits of infinite ion Reynolds number and infinite negative probe potential are taken, and use is made of the method of matched asymptotic expansions.[21] The ion flow near the leading edge of this type of sheath was considered by Dukowicz,[22] who used a numerical scheme to solve the appropriate partial differential equations for various choices of dimensionless parameters. The case of a thick sheath around a cylindrical probe transverse to a low speed flow was considered in an approximate fashion by Kulgein,[23] and reconsidered by de Boer and David.[24]

The present work contains, in addition to the case of a high-speed, free molecular plasma mentioned before, a group of problems in high-speed continuum plasmas where the sheath is thick compared with the viscous boundary layer. This group includes the problem considered in Refs. 20 and 21. It is shown that this problem is amenable to solution by a method of integral relations which takes account of convective effects within the sheath. Using either this method or the method of Ref. 20, we study flat-plate and cylindrical probes aligned parallel to the flow. In all cases, the negative potential applied to the probe as well as the ion Reynolds number are assumed to be large.

II. Flat-Plate Probe in Continuum Regime

We first consider the ion boundary layer that forms over a flat-plate probe immersed in a slightly ionized continuum flow, with the probe aligned parallel to the flow (see Fig. 1). The temperature T of the neutral component is assumed constant. The ion temperature T_i is assumed equal to T, while the electron temperature T_e is assumed to be a constant of order T. It is assumed that there is no secondary ionization, and no emission of electrons from the surface. Magnetic effects are neglected. All ions reaching the probe are assumed to be neutralized by recombination with electrons from the surface. Only one species of singly charged ions is assumed present, and their electric mobility is assumed constant. The ion number density N_i and electron number density N_e in the freestream are taken equal to a constant number density N_0. Assuming a steady state, without production or recombination of charged particles, the basic equations describing the problem are[21]

$$\nabla\cdot(N_\alpha \vec{u}_\alpha) = 0 \tag{1}$$

$$\vec{u}_\alpha = \vec{u} - D_\alpha \nabla \ln p_\alpha - K_\alpha \nabla V \tag{2}$$

$$\nabla^2 V = -e(N_i - N_e)/\varepsilon_0, \tag{3}$$

where D = diffusion coefficient, $K = eD/(kT)$ = mobility, e = ionic charge, k = Boltzmann's constant, V = electrostatic potential, ε_0 = dielectric constant for vacuum, and p = pressure. Subscript α denotes either ions (i) or electrons (e). Equation (1) is the continuity equation for the charged particles, (2) is a simplified momentum equation, and (3) is the Poisson equation. We set

$$\begin{aligned} &\phi = V/V_w, && h_i = (\varepsilon_0 kT/N_0 e^2)^{1/2} \\ &\omega = -eV_w/(kT), && R_i = Uh_i/D_i \\ &n = N_i/N_0, && \xi = x/(h_i R_i) \\ &\vec{u} = u\vec{v}, && \eta = y/(h_i \omega^{1/2}) \\ & && \varepsilon = \partial\phi/\partial\eta \end{aligned} \tag{4}$$

Here, R_i is the ion Reynolds number, ε is the nondimensionalized vertical component of the electric field, and subscript w denotes quantities evaluated at the wall. Taking the limit $R_i \to \infty$, $\omega \to \infty$, with $\omega^{1/2}/R_i \to 0$ leads to the sheath equations[21]

$$n_\xi + (n\varepsilon)_\eta = 0 \tag{5}$$

Received August 26, 1971; revision received January 24, 1972. The authors wish to thank D. L. Turcotte for a number of helpful discussions. This work was supported in part by the United States Office of Naval Research.

Index categories: Plasma dynamics and MHD; Research Facilities and Instrumentation.

* NASA Trainee, Graduate School of Aerospace Engineering; now at AVCO Systems Division, Wilmington, Mass.

† Associate Professor, Graduate School of Aerospace Engineering. Associate Fellow AIAA.

$$\varepsilon_\eta = n \tag{6}$$

and to the outer region solution[21]

$$\varepsilon = 0, \qquad n = 1 \tag{7}$$

Terms of order $\beta = D_i T_e/(D_e T_i)$ have been neglected in Eqs. (5–7). Subscripts ξ and η denote partial differentiations with respect to ξ and η, respectively. Equation (5) is the result of substituting (2) into (1), while (6) is the form of the Poisson equation valid in the sheath. The outer region and the ion sheath are separated by a transition region, which to lowest order in β simply is a line. We call this line the edge of the sheath, and denote its vertical coordinate by $\eta_s(\xi)$ (see Fig. 1). The boundary conditions which the solution of (5) and (6) should satisfy are[21]

$$\begin{aligned} n_s &\equiv n(\xi,\eta_s) = 1, \qquad \varepsilon_s \equiv \varepsilon(\xi,\eta_s) = 0 \\ \phi_s &\equiv \phi(\xi,\eta_s) = 0, \qquad \phi_w \equiv \phi(\xi,0) = 1 \quad (\xi > 0) \end{aligned} \tag{8}$$

Substitution of (6) into (5), and integration with respect to η up to the sheath edge leads to

$$\varepsilon_{\xi s} - \varepsilon_{\xi w} = (n\varepsilon)_w = j(\xi) \tag{9}$$

where subscript s denotes conditions evaluated at the sheath edge. Equation (9) yields the nondimensionalized current density at the wall $j(\xi)$, provided we can express $\varepsilon_{\xi s}$ and $\varepsilon_{\xi w}$ as functions of j. We do this in an approximate fashion by considering an equivalent one dimensional situation, i.e., a situation in which the derivative with respect to ξ is zero. From (5) and (6) we find

$$\begin{aligned} n &= -2^{-1/2} j (j\eta + C_1)^{-1/2}, \quad \varepsilon = -2^{1/2}(j\eta + C_1)^{1/2} \\ \phi &= -2^{3/2}(3j)^{-1}(j\eta + C_1)^{3/2} + C_3 \end{aligned} \tag{10}$$

as our approximate profiles. We determine C_1 as function of η_s and j by using the first of boundary conditions (8)

$$C_1 = \tfrac{1}{2} j^2 - j\eta_s$$

It follows that

$$\varepsilon = -[2(j\eta + \tfrac{1}{2}j^2 - j\eta_s)]^{1/2}$$

$$\varepsilon_{\xi s} = (d/d\xi)(j - \eta_s) \tag{11}$$

$$\varepsilon_{\xi w} = (d/d\xi)\varepsilon_w = (d/d\xi)(j^2 - 2j\eta_s)^{1/2} \tag{12}$$

Using the last two conditions of (8), we find

$$\eta_s = \tfrac{1}{2} j [1 - (1 + 3/j^2)^{2/3}] \tag{13}$$

The approximate profile cannot simultaneously satisfy the first and the second of conditions (8), and we drop the second. Substituting (11–13) into (9), we obtain

$$(d/d\xi)\{j[\tfrac{1}{2} - (1+3/j^2)^{1/3} + \tfrac{1}{2}(1+3/j^2)^{2/3}]\} = j \tag{14}$$

The leading edge solution of (13) and (14) can be found by letting $-j \gg 1$, which gives

$$j = -(3/8\xi)^{1/4}, \qquad \eta_s = (8\xi/3)^{1/4} \tag{15}$$

The large ξ solution is obtained by letting $-j \ll 1$, leaving

$$j = -3^{1/2}(8\xi)^{-3/4}, \qquad \eta_s = (9\xi/2)^{1/4} \tag{16}$$

Expressions (16) agree with the leading terms of the corresponding results (49) and (46) of Ref. 21, and are identical to the results for j and η_s obtained using the quasi-one-dimensional method.[20]

The integration of (14) can be carried out in closed form. For practical reasons, it was found convenient to integrate (14) numerically using a four point Runge-Kutta scheme. It is interesting to compare the results obtained for the dimensionless current

$$\mathcal{J}(\xi) \equiv \int_0^\xi j(\xi')\, d\xi'$$

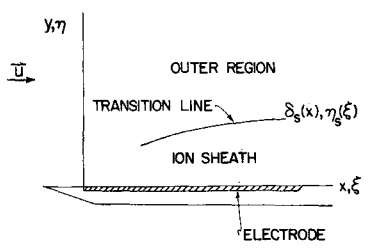

Fig. 1 Sketch of flat-plate probe geometry.

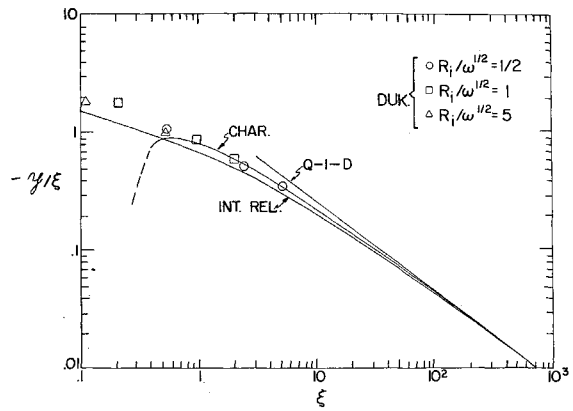

Fig. 2 The quantity $-\mathcal{J}/\xi$ as function of ξ, for flat-plate probe. Curves represent results of the quasi-one-dimensional method of Ref. 20 (Q-1-D); of the method of characteristics as given by (50) of Ref. 21 up to the logarithmic term (char.); and of the method of integral relations as determined by (14). Points are numerical results of Ref. 22.

to those of Refs. 21 and 22 (see Fig. 2). In Ref. 22, numerical calculations are described which were based on the present equations (1–3), with the diffusion term in (2) set equal to zero. The calculations were carried out for various values of the parameter $R_i/\omega^{1/2}$. In the present work, this parameter was taken to be infinitely large, which made it possible to neglect derivatives with respect to x compared with corresponding derivatives with respect to y. Such neglect is justified for any value of $R_i/\omega^{1/2}$ sufficiently far downstream. Indeed, the present result for $\mathcal{J}$ is seen to agree with that of Ref. 22 at large ξ (Fig. 2). As a matter of fact, there is quite good agreement with the numerical calculations even when ξ is as small as 0.1, and the numerical results show only a slight dependence on the value of $R_i/\omega^{1/2}$. This means that "leading edge effects" are not important, as far as the results of the present method are concerned. From a practical point of view, this gives the present method an advantage over the method of Ref. 21. Another practical advantage is the far greater simplicity of the present method, which makes it suitable for application to geometries more complicated than the flat plate.

III. Cylindrical Probe in Continuum Regime

Cylindrical probes aligned parallel to the flow have been used by various experimenters. The probes consist of solid circular cylinders, usually made of thin wire, with an appropriate electrical bias. Even though the mathematical details are somewhat more complicated, the theory for these probes can be given in a manner similar to the integral method used for the flat plate.

Using the cylindrical coordinate system shown in Fig. 3, the axisymmetric equivalent of (5) and (6) is

$$\begin{aligned} n_\xi + \rho^{-1}(\rho n\varepsilon)_\rho &= 0 \\ \rho^{-1}(\rho\varepsilon)_\rho &= n \end{aligned} \tag{17}$$

where $\rho = r/(h_i\omega^{1/2})$ and $\varepsilon = \phi_\rho$; subscript ρ denotes partial differentiation with respect to ρ. After performing an analysis completely analogous to that used for the flat plate, the governing equations corresponding to (13) and (14) are found to be

$$\ln\left\{\frac{(-C)^{1/2} + (\sigma_s^2 - C)^{1/2}}{\sigma_s[(\sigma_s^2 - C - 1)^{1/2} + (\sigma_s^2 - C)^{1/2}]}\right\} + \frac{(\sigma_s^2 - C - 1)^{1/2} - (-C)^{1/2}}{(\sigma_s^2 - C)^{1/2}} + \frac{\mathcal{V}}{(-C\sigma_s^2 + C^2)^{1/2}} = 0 \tag{18}$$

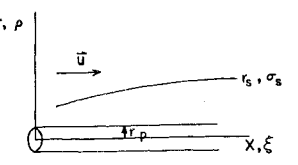

Fig. 3 Coordinate system for cylindrical probe.

$$\frac{dC}{d\xi}+\frac{d}{d\xi}(C^2+C-C\sigma_s^2)^{1/2}-\sigma_s\frac{d\sigma_s}{d\xi}=C, \tag{19}$$

where $\sigma_s=\rho_s/\rho_p$, $C=(n\varepsilon)_p/\rho_p=-j_p/\rho_p$, $\mathscr{V}=1/\rho_p^2$, while the subscript p denotes conditions evaluated at the probe surface ($r=r_p$).

Near the leading edge, $\sigma_s\to 1$ and $-C\gg 1$, which gives

$$-C=-\mathscr{V}/\ln\sigma_s,\quad \sigma_s-1=(8\mathscr{V}\xi/3)^{1/4} \tag{20}$$

It can be shown that these results agree with the flat plate results near the leading edge. This is to be expected because the curvature effects vanish in this region where $\delta_s=r_s-r_p\to 0$. The downstream asymptotic solution may be found by assuming $-C\ll 1$ and $\sigma_s\gg 1$ which leads to

$$\begin{gathered}-C=\mathscr{V}\sigma_s^{-2}[\ln(2\sigma_s)-1]^{-2},\\ \sigma_s^4[(\ln 2\sigma_s)^2-\tfrac{5}{2}\ln(2\sigma_s)+\tfrac{13}{8}]=4\mathscr{V}^2\xi\end{gathered} \tag{21}$$

In order to obtain a solution valid over the entire range of ξ, (18) and (19) were solved numerically using (20) to start the solution at small ξ. The current density-sheath thickness relation (18) could not be solved explicitly for the current density in terms of the sheath thickness as in the flat-plate case. Hence, a Newton-Raphson iterative scheme was used to solve (18) for $C(\sigma_s, \mathscr{V})$, while (19) was simultaneously integrated numerically in the downstream direction by means of Simpson's rule.

A plot of numerical results for $\sigma_s(\xi)$ at various values of the parameter $\mathscr{V}$ is shown in Fig. 4, while Fig. 5 shows $-j_p/\rho_p$. We note that $\mathscr{V}$ is proportional to the voltage V_w. The large ξ results are found to approach those given by Eq. (21), thus providing a check on the numerical integration. It is interesting to note that, for given flow conditions and electrode potential, the flat-plate sheath is thicker than the equivalent axisymmetric sheath. This can be seen by comparing the quantity:

$$\eta_s/\rho_p=\mathscr{V}^{1/2}(9\xi/2)^{1/4} \tag{22}$$

with σ_s-1, where σ_s is the result shown in Fig. 4. The difference is explained by the better shielding in the axisymmetric case, which results from the convergence of the ion streamlines on the probe.

IV. Viscous Boundary-Layer Effects

In any practical situation, neither the Reynolds number R_i nor the electrostatic potential parameter ω can be infinitely large. As a consequence it may be necessary to apply corrections to the results obtained in the previous sections.

It appears that the main corrections which must be considered are those arising from the presence of a viscous boundary layer. This boundary layer modifies both the convection velocity u, as well as the ion mobility K_i. Langevin's theory for ionic mobility predicts $K_i=K_0\rho_0/\rho$ where K_0 is the "reduced" mobility, (i.e., mobility at some standard temperature and pressure), ρ_0 is some standard density, and ρ is actual density.[25] The experiments of interest in this study typically involve the hot flow

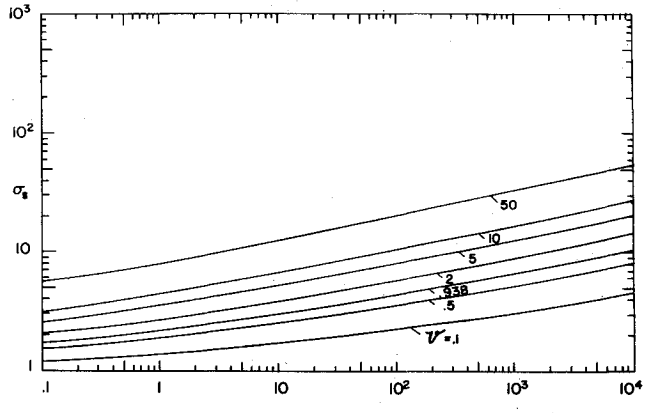

Fig. 4 Nondimensionalized sheath thickness σ_s as function of ξ at various values of $\mathscr{V}=\rho_p^{-2}$, for axisymmetric probe in continuum regime.

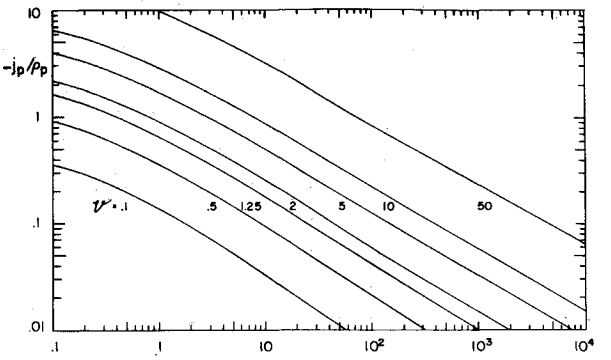

Fig. 5 Nondimensionalized current density $-j_p/\rho_p$ as function of ξ at various values of $\mathscr{V}=\rho_p^{-2}$, for axisymmetric probe in continuum regime.

of an ionized gas over a cold electrode with a cool viscous boundary layer adjacent to the electrode. This reduces the mobility in the inner portion of the sheath and thus leads to a decrease in the current collected. It can easily be shown that the results obtained previously for J yield $J(L)\propto K_i^{1/4}$, where $J(L)$ denotes the current collected per unit width by an electrode of length L. In view of the small dependence of J on K evidenced here, it may be expected that the reduction in current collected will be relatively small.

When the viscous boundary-layer thickness δ_0 becomes larger than the sheath thickness δ_s, the convection velocity at the outer edge of the sheath is reduced from its freestream value. Hence, the current is decreased below that predicted by the reduced mobility theory just outlined. In the present section an estimate is given for the reduction in current caused by both these effects. Most of the attention is confined to the case of a flat plate.

It was found in Sec. II that for the flat plate the results obtained using the quasi-one-dimensional (Q-1-D) method of Ref. 20 agree with the downstream results obtained from the method of integral relations and from the method of characteristics. Since the Q-1-D theory is mathematically much simpler than the other theories, we adopt it for the present problem.

As discussed in Ref. 20, the equation expressing continuity of ions crossing the sheath edge is

$$f=-eu_sN_0\,d\delta_s/dx \tag{23}$$

where f is the ion flux or current density, and u_s is the component of convective velocity at the outer edge of the sheath. We find another relation between f and δ_s by using

$$\begin{gathered}eN_iv_i=f\\ N_i=\varepsilon_0e^{-1}\partial E/\partial y,\quad v_i=K_iE\end{gathered} \tag{24}$$

Assuming the density profile in the viscous boundary layer to be known, K_i is a given function of x and y. Combining Eqs. (24) results in

$$\partial E^2/\partial y=2f/[\varepsilon_0K_i(x,y)] \tag{25}$$

Since K_i is not constant, we cannot integrate this expression analytically as before. Applying the boundary conditions $E(\delta_s)=0$, $V(\delta_s)=0$, $V(0)=V_w$ to (25) and using (23) results in

$$\frac{d\eta_s}{d\xi}=\frac{1}{2\bar{u}_s}\left\{\int_0^{\eta_s}\left[\int_{\eta'}^{\eta_s}\frac{d\eta''}{\bar{K}(\xi,\eta'')}\right]^{1/2}d\eta'\right\}^{-2} \tag{26}$$

where $\bar{K}=K_i/K_0$ is the nondimensionalized mobility and $\bar{u}_s=u_s/u_0$ the nondimensionalized convective velocity at the sheath edge. Subscript 0 again refers to freestream conditions. We use $E(\delta_s)=0$ instead of $N_i(\delta_s)=N_0$ as the first boundary condition because it simplifies the algebra considerably, while these two boundary conditions give the same relation between δ_s and f at large ξ. To find expressions for the mobility $\bar{K}(x,y)$ and the velocity $\bar{u}_s(x,y)$, we considered the compressible boundary layer equations for flow over a flat plate at a temperature T_w. Following von Kármán and Tsien[26] and Pohlhausen,[27] we found the temperature and hence mobility profile in the boundary layer by using a momentum integral technique,

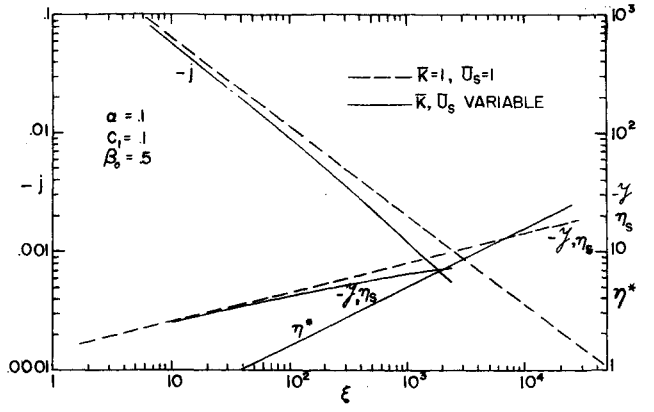

Fig. 6 Nondimensionalized current density $-j$, current $-\mathscr{J}$, sheath thickness η_s, and viscous boundary-layer thickness η^* as function of ξ.

for $\alpha \equiv T_w/T_0 = 0.1,\ 0.2$ and for various values of $\beta_0 = \frac{1}{2}(\gamma-1)M_0^2$. The double integration in (26), based on these profiles of K, was performed using Simpson's rule, starting at the leading edge and marching downstream. It appeared from the results that the reduction in current collected is less than about 5% provided the displacement thickness of the viscous boundary layer is less than about $\frac{1}{3}$ of the sheath thickness at the end of the electrode. Figure 6 shows the results for a typical case considered: $\alpha = 0.1, C_1 \equiv (\mu_w\rho_w)(\rho_0^2 D_0\,\omega)^{-1} = 0.1$ and $\beta_0 = 0.5$. For $\eta^* \equiv \delta^* h_i^{-1}\omega^{-1/2} = 0.7\eta_s$ the current density $j = -d\eta_s/d\xi$ is reduced by about 30%, and the current $-\mathscr{J}$ by about 15%, compared with the uncorrected results denoted by dotted lines.

In order for the viscous boundary-layer effects discussed in this section to remain small, we can use the general criterion $\delta^* < \delta_s$. For the flat plate this condition may be approximated by

$$\xi^{1/2} < \omega$$

assuming that the viscous boundary layer and the sheath have a common leading edge. This condition on ξ arises from the circumstance that the sheath grows as $x^{1/4}$, while the boundary layer grows as $x^{1/2}$.

Using a similar treatment for the axisymmetric geometry, we have found that the results of Sec. III are not affected very much by viscous boundary layer effects provided $\xi^{1/2} < \omega \ln(4\xi h_i^2/r_p^2)$.

The influence of ion production inside the sheath was considered in Ref. 28.

V. Free Molecular Ion Boundary Layers

Several investigators[2-4,6,7] recently have used cylindrical probes in flowing gases under free molecular conditions. For probes aligned with the flow, it was found that, under certain conditions, the experimental current was greater than that predicted by conventional theories, which do not take account of the presence of the flow. In the present section, a theory is developed which accounts for the influence of the flow. Results are presented for the flat plate geometry, as well as for the axisymmetric case.

For the free molecular case, the ion sheath thickness is small compared with an ion-neutral mean free path λ_{in}. We are not restricted to a slightly ionized flow but require $-V_w \gg kT_e/e$ so that we can approximate the potential drop across the sheath as V_w. We do not have to consider viscous boundary-layer effects since the mean free path is large, and the freestream is assumed uniform. In other respects, the assumptions are the same as in the continuum case. Application of the integral method of Sec. II to the present case leads to an unacceptable singularity at the leading edge.[29] We can avoid this difficulty by reverting to the quasi-one-dimensional method. In order to obtain the conventional or Langmuir solution for the downstream region, a term representing the thermal flux of ions crossing the outer edge of the sheath must be included in the "global" ion conservation relation.

A. Flat Plate

The "global" ion conservation equation is

$$-f(x) = euN_0\,d\delta_s/dx + f_r \tag{27}$$

where f_r is the thermal flux crossing the sheath edge (we take $f_r > 0, f < 0$). We assume that this thermal flux consists of monoenergetic ions, all entering the sheath with perpendicular velocity $v_0 = f_r/(eN_0)$. Equation (27) is supplemented by an approximate relation between δ_s and f, for which we use the Child-Langmuir law for space-charge limited current for the case with initial velocity v_0:

$$-f/f_r = \hat{\eta}_s^{-2} \tag{28}$$

where

$$\hat{\eta}_s = \delta_s[2\mathscr{V}_0 h_i W^{1/2}(1+\tfrac{1}{3}W)]^{-1}$$
$$W = (1+\omega/\mathscr{V}_0^2)^{1/2} - 1, \quad \mathscr{V}_0^2 = \tfrac{1}{2}mv_0^2/(kT_i)$$

Substituting (28) into (27) and integrating, we obtain

$$\tfrac{1}{2}\ln[(1+\hat{\eta}_s)/(1-\hat{\eta}_s)] - \hat{\eta}_s = \hat{x} \tag{29}$$

where $\hat{x} = xv_0[2h_i W^{1/2}(1+\frac{1}{3}W)\mathscr{V}_0 u]^{-1}$, and where the constant of integration was determined from the condition $\hat{\eta}(0) = 0$. Equations (29) and (28) provide $\hat{\eta}_s$ and $-f/f_r$ as function of $\hat{x}$. For large $\hat{x}$, the limiting solution is

$$\hat{\eta}_s = 1, \qquad -f/f_r = 1, \tag{30}$$

while for small $\hat{x}$

$$\hat{\eta}_s = (3\hat{x})^{1/3}, \qquad -f/f_r = (3\hat{x})^{-2/3} \tag{31}$$

The quantity $-f/f_r$ is plotted in Fig. 7 as function of $\hat{x}$. It is seen that for

$$\hat{x} < \hat{x}_c \approx 1/3$$

there is a considerable increase in the current density collected at the probe arising from convective effects.

Provided the electron temperature T_e is not larger than the ion temperature T_i, so that there are no complications arising from Bohm's sheath criterion, we can relate v_0 to T_i by $v_0 = \frac{1}{4}(8kT_i/\pi m_i)^{1/2}$. For this case, $\mathscr{V}_0^2 = (4\pi)^{-1}$. In the limit $W \to \infty$, (30) now gives back the conventional Langmuir result. For the case $T_i < T_e$, $\mathscr{V}_0^2$ is of order $(4\pi)^{-1}T_e/T_i$ (see also Sec. VI).

B. Cylindrical Probe

The global ion conservation equation now is (cf. Fig. 3)

$$-\kappa = \mu\sigma_s\,d\sigma_s/d\tilde{\xi} + \sigma_s \tag{32}$$

where $\kappa \equiv (N_i v_i)_p/N_0 v_0$ (<0) is the nondimensionalized current density at the probe surface. Furthermore $\sigma_s = r_s/r_p$ and $\tilde{\xi} = x/r_p$, r_p being the radius of the probe. The quantity $\mu \equiv u/v_0$ is proportional to the Mach number of the free stream. As an approximate relation between sheath thickness and current density we use the well-known result of Langmuir and Blodgett[30]

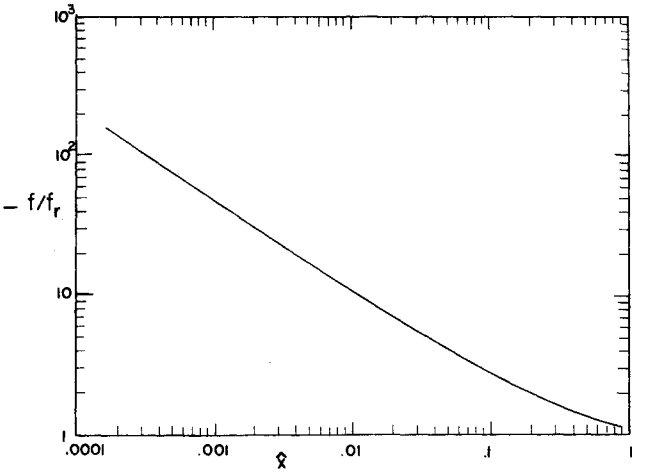

Fig. 7 Nondimensionalized current density $-f/f_r$ as function of $\hat{x}$, for flat-plate probe in free molecular regime.

$$-\kappa = Q^{-1}\beta_p^{-2} \tag{33}$$

with

$$Q = 9\mathscr{V}_0 r_p^2/(4h_i^2\omega^{3/2}), \quad \mathscr{V}_0^2 = \tfrac{1}{2}mv_0^2/kT_i$$

$$\beta_p^2 = (\gamma + 0.4\gamma^2 + 0.091\gamma^3 + 0.014\gamma^4 + 0.002\gamma^5 + \ldots)^2, \quad \sigma_s < 10$$

$$\beta_p^2 \approx 4.67\sigma_s[\ln(2^{-1/2}\sigma_s)]^{3/2}, \quad \sigma_s > 10$$

where $\gamma = \ln\sigma_s$. Combining (32) and (33) produces

$$d\sigma_s/d\tilde{x} = \sigma_s^{-1}\beta_p^{-2} - Q \tag{34}$$

where $\tilde{x} = \tilde{\xi}\mu^{-1}Q^{-1}$. The limiting downstream solution is

$$\sigma_s\beta_p^2 Q = 1, \qquad -\kappa/\sigma_s = 1 \tag{35}$$

which is just the conventional Langmuir result. Solving (34) and (33) for small $\tilde{x}$ gives

$$\sigma_s - 1 = (3\tilde{x})^{1/3}, \qquad -\kappa/\sigma_s = Q^{-1}(3\tilde{x})^{-2/3} \tag{36}$$

As ought to be the case, these results agree with the flat plate results (31) in the limit of large W. Results for $-\kappa/\sigma_s$ as a function of $\tilde{x}$ for various Q are shown in Fig. 8. Again, there is an important increase in $-\kappa/\sigma_s$ arising from convective effects for small $\tilde{x}$. A typical value $\tilde{x}_c$ below which convective effects must be taken into account can be obtained by equating the second of (35) to the second of (36), which gives

$$\tilde{x}_c \approx \tfrac{1}{3}Q^{-3/2} \tag{37}$$

In deriving the results of this section we have tacitly assumed that the effects of angular momentum of the ions may be left out of account. Such effects may cause the current to be limited by orbital motion rather than by space charge effects. The orbital motion limitation would make itself felt most strongly in the downstream region. Langmuir and Mott-Smith[31] indicate that in this region orbiting effects are negligible within 5% provided $\omega^{1/2}/\sigma_s \geqq 2$ where $\sigma_s^2 \gg 1$.

VI. Comparison with Experiment

This section is devoted to comparing the results obtained with available experimental data. Unfortunately, not many data are available that clearly lie in regimes where our theory is valid. This is largely because most experimenters deliberately worked in regimes where flow effects supposedly were not important, and where existing no-flow theories could be used to interpret their data. Nevertheless, we find that taking account of flow effects explains some results that were previously not well understood.

Experimental results with free molecular ion-density probes have been obtained by Lederman, Bloom, and Widhopf.[6] By shocking air and then expanding it through a nozzle, they were able to obtain flows that were freemolecular with respect to the diameter of thin cylindrical probes aligned parallel with the flow. They applied negative voltages to the probes so as to collect ions. The existence of flow effects in their experiment is clear from Fig. 9 of Ref. 6, which is a plot of current density averaged over the probe, versus length to diameter ratio L/d of the probe. The normalized current density increases as L/d decreases, showing a dependence of current density on the streamwise coordinate, and therefore a flow effect. Lederman et al.[6] concluded that L/d must be greater than 225 for the current density to be practically independent of L/d for their experimental conditions.

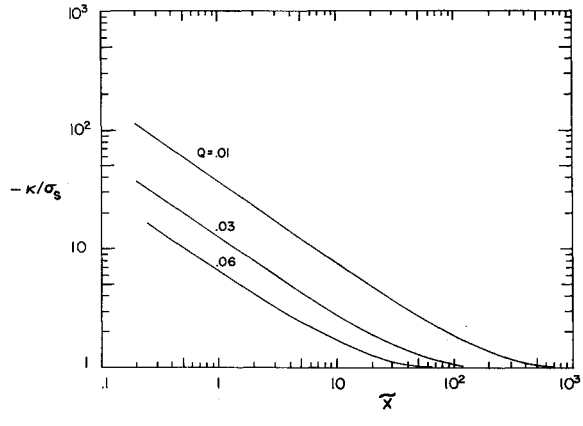

Fig. 8 Nondimensionalized current density $-\kappa/\sigma_s$ as function of $\tilde{x}$ at various Q, for cylindrical probe in free molecular regime.

For purposes of comparison with the theory of Sec. V.B, it is convenient to use Fig. 7d of Ref. 6, which gives a curve of best fit through the experimental data[6] (see Fig. 9). The coordinates of this plot are α_p and r_p/h_e, and the curves shown are for $\tilde{\omega} = 35$, 23.4, and 11.7. Here

$$h_e = (\varepsilon_0 kT_e/N_0 e^2)^{1/2}, \quad \tilde{\omega} = -eV_w/(kT_e), \quad \alpha_p = f_i/(eN_0 v_0')$$

where f_i is the current density averaged over the entire surface of the probe, and $v_0' = (kT_e/2\pi m_i)^{1/2}$.

It is readily shown that in the present notation, $\alpha_p = 1.52\langle\kappa\rangle$, where $\langle\ \rangle$ denotes an average taken over the length of the probe. Since the electron temperature T_e was much larger than the ion temperature T_i in the experiments of Ref. 6, μ^{-1} in the present theory was taken to be $u^{-1}(kT_e/2.7m_i)^{1/2}$. This is of the order of v_0'/u, and is an expression derived by Schulz and Brown,[32] who considered cylindrical probes in the absence of flow. The numerical factor in the expression just given must be considered somewhat uncertain. Fortunately, the total current collected by a cylindrical probe is not very sensitive to this factor. As can be seen from Fig. 9, the present theoretical results calculated for $L/d = 50$ agree very well with the experimental data. The agreement appears to be within 15% over a $\tilde{\omega}$ range from 11.7 to 35 and a r_p/h_e range from 0.2 to 2.3, which is within the experimental scatter of about 20%.

Also shown in Fig. 9 are theoretical results based on the work of Laframboise,[33] as given in Ref. 6, and on the work of Langmuir and Blodgett.[30] Neither of these theories takes account of flow effects. Except for large r_p/h_e, Laframboise's theory is not strictly applicable, because the experimental conditions were such that the sheath was not completely collisionless. The collisions of importance were ion-neutral collisions, whereas ion-ion collisions played only a minor role. The collisions tend to remove the orbital motion limitation, and hence lead to an increase in the current collected.[6] In view of this, it is more appropriate to use the results of Langmuir and Blodgett[30] already mentioned in Sec. V.B. Comparison of the present results with those based on Ref. 30 allows a direct evaluation of the importance of flow effects in the experiments of Ref. 6. It is seen that for $\alpha_p \approx 30$, convection allows for about 50% of the total current. We find that for this value of α_p, the ratio of $\tilde{x}_c$ to the nondimensionalized length $\tilde{x}_L = L/(r_p\mu Q)$ given by

$$\tilde{x}_c/\tilde{x}_L \approx 0.34(-eV_w/kT_e)^{3/4}(h_e/L)(u/v_0)$$

is of the order of $\frac{1}{2}$. For decreasing values of α_p, the influence of convection on the total current is seen to be smaller. It should be mentioned that the current convected into the frontal areas of the probe is negligible (less than a few percent) for all the experimental results discussed in this section.

Another series of experiments with small cylindrical probes aligned parallel to the flow was reported by Sonin.[5] No flow effects were found for L/d as small as 100. This is consistent with (37), which gives $\tilde{x}_c/\tilde{x}_L \approx 0.03$ for the conditions of Ref. 5, indicating that flow effects should be very small. In agreement with the results of Ref. 6, it was found that α_p is larger than predicted by Laframboise's theory for $r_p/h_e < 3$. While the ratio of sheath thickness to ion-neutral mean free path was large, the ion-ion mean free path was small (0.03–0.5 times the probe diameter d). The explanation for the difference in α_p's is believed to be the removal of the orbital motion limitation by ion-ion collisions inside the sheath.

Finally, we mention the experiments of Dunn and Lordi.[7] These experiments were rather similar to those of Refs. 5 and 6; however, no significant increase in current was found over the values predicted by Laframboise's theory. In the work of Ref. 7, r_p/h_e was of order 1, $\tilde{\omega}$ was of order 15, and L/d equalled 50. The value of α_p predicted from Laframboise's theory is 4.37. This quantity is a measure for the ratio of sheath radius r_s to probe radius r_p. The ion-neutral mean free path λ_{in} amounted

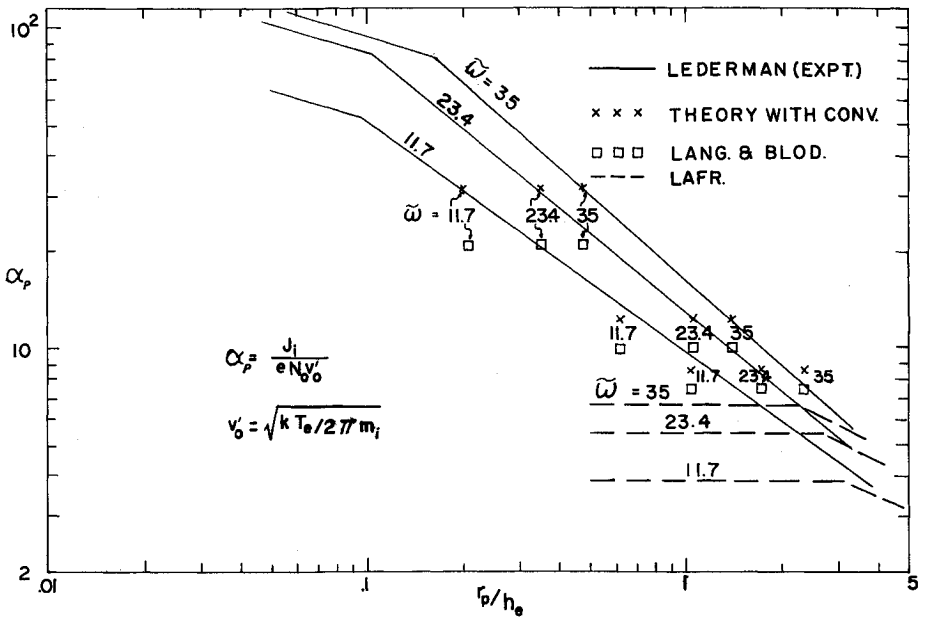

Fig. 9 Comparison of experimental results of Ref. 6 with theory, as discussed in Sec. VI.

to less than $2r_p$. Consequently, the ratio λ_{in}/r_s was less than $\frac{1}{2}$, which is significantly smaller than the corresponding value in the work of Ref. 5 ($\lambda_{in}/r_p \gtrsim 8$). We conclude that in the work of Ref. 7, collisions not only constituted an orbital motion limitation, but also were sufficiently numerous to reduce the current collected by the probes. In this sense, the agreement of the experimental results of Ref. 7 with Laframboise's theory must be considered fortuitous. In view of the sizeable number of collisions with neutrals suffered by ions in the sheath, the most appropriate theory for evaluating the experimental data is the continuum theory of the present Sec. III. To this purpose, we used the Einstein relation $K_i = eD_i/(kT_i)$, and set $D_i = \frac{1}{3}a_i\lambda_{in}$, where a_i is the ion sound speed. This yielded sheath thicknesses at the end of the probe of about 6–12 times the probe radius, and values of N_0 which are up to 20% higher than the Laframboise values for most of the downstream stations ($A/A^* = 295$, 250, and 210), and about a factor 2 higher at the other stations ($A/A^* = 114$ and 235). The new values of N_0 agree with the microwave results of Ref. 7, within experimental scatter and uncertainty.

VII. Concluding Remarks

In the previous pages, we have formulated theories for ion boundary layers, which are useful for the interpretation of data obtained with negatively biased electric probes immersed in flowing plasmas. While a number of simplifying assumptions has been made, it is believed that the results allow the determination of freestream ion density typically within a factor of two, and in some cases with accuracies of up to 10–20%, say. One of the simplifying assumptions made for the continuum case is the constancy of ion mobility. Actually, the mobility is constant only when the density is constant, and when the electric field E is small. The effect of density was investigated in Sec. IV, and was found to be small. Similarly, it may be predicted that variations of mobility from its low E value will not greatly change the results obtained. An idea of the size of such variations may be gained from Ref. 25, Chap. I, Pt. two, Sec. 8; generally, they are not very large.

For the flat-plate case, one of the conclusions reached is that the quasi-one-dimensional method of Ref. 20 correctly gives the leading term in the expression for the current collected, and for the sheath thickness. In view of its simplicity, the quasi-one-dimensional method is attractive for finding results in more complicated cases. It was used in Sec. IV for investigation of the influence of the viscous boundary layer, and in Sec. V for treating free molecular probes.

The results obtained in Sec. V for the free molecular case are applicable when the convective velocity is much larger than the average thermal velocity, i.e., when the ion flow is hypersonic. Convenient criteria for estimating the importance of flow effects are given by the relation following (31) and by (37) or its modified form given in Sec. VI. The theory of Sec. V may also be applied to electron collection provided the electron flow is hypersonic, a situation which is seldom encountered. It is important to note that none of the results obtained for the continuum regime may be applied to electron collection. For ion collection in the continuum regime, we have shown that the influence of the viscous boundary layer can be made small. The presence of the flow then permits a simple and straightforward interpretation of experimental probe data.

References

[1] Chen, F. F., *Plasma Diagnostic Techniques*, edited by R. H. Huddlestone and S. L. Leonard, Academic Press, New York, 1965, Chap. 4.

[2] Talbot, L., "Theory of the Stagnation-Point Langmuir Probe," *The Physics of Fluids*, Vol. 3, No. 2, March 1969, pp. 289–298; also *The Physics of Fluids*, Vol. 5, No. 5, May 1962, pp. 629–630.

[3] Sonin, A. A., "Free-Molecular Langmuir Probe and its Use in Flowfield Studies," *AIAA Journal*, Vol. 4, No. 9, Sept. 1966, pp. 1588–1596.

[4] Graf, K. A. and deLeeuw, J. H., "Comparison of Langmuir Probe and Microwave Diagnostic Techniques," *Journal of Applied Physics*, Vol. 38, No. 11, Oct. 1967, pp. 4466–4472.

[5] Sonin, A. A., *Journal of Geophysical Research*, Vol. 72, No. 17, 1967, pp. 4547–4557.

[6] Lederman, S., Bloom, M. H., and Widhopf, G. F., "Experiments on Cylindrical Electrostatic Probes in Slightly Ionized Hypersonic Flow, *AIAA Journal*, Vol. 6, No. 11, Nov. 1968, pp. 2133–2139.

[7] Dunn, M. G. and Lordi, J., "Measurement of Electron Temperature and Number Density in Shock-Tunnel Flows, Part I: Development of Free-Molecular Langmuir Probes," *AIAA Journal*, Vol. 7, No. 8, Aug. 1969, pp. 1458–1465.

[8] Stahl, N. and Su, C. H., "Theory of Continuum Flush Probes," *The Physics of Fluids*, Vol. 14, No. 7, July 1971, pp. 1366–1376.

[9] Turcotte, D. L. and Gillespie, J., "Electrical Resistance and Sheath Potential Associated with a Cold Electrode," *AIAA Journal*, Vol. 1, No. 10, Oct. 1963, pp. 2293–2299.

[10] Lam, S. H., "A General Theory for the Flow of Weakly Ionized Gases," *AIAA Journal*, Vol. 2, No. 2, Feb. 1964, pp. 256–262.

[11] Chung, P. M., "Weakly Ionized Nonequilibrium Viscous Shock Layer and Electrostatic Probe Characteristics," *AIAA Journal*, Vol. 5, No. 5, May 1965, pp. 817–825.

[12] Pollin, I., "Stagnation Point Langmuir Probe in a Shock Tube—Theory and Measurements," *The Physics of Fluids*, Vol. 7, No. 9, Sept. 1964, pp. 1433–1445.

[13] Su, C. H., "Compressible Plasma Flow over a Biased Body," *AIAA Journal*, Vol. 3, No. 5, May 1965, pp. 842–848.

[14] Chung, P. M. and Blankenship, V. P., "Theory of Electrostatic Double Probe Comprised of Two Parallel Plates," *AIAA Journal*, Vol. 4, No. 3, March 1966, pp. 442–450.
[15] Bredfeldt, H. R., Scharfman, W. E., Guthart, H., and Morita, T., "Boundary-Layer Ion Density Profiles as Measured by Electrostatic Probes," *AIAA Journal*, Vol. 5, No. 1, Jan. 1967, pp. 91–98.
[16] Grey, J. and Jacobs, P. F., "Cooled Electrostatic Probe," *AIAA Journal*, Vol. 5, No. 1, Jan. 1967, pp. 84–90.
[17] Hoppmann, R. F., "Cold-Electrode Characteristics in Shock-Ionized Air Plasmas," *The Physics of Fluids*, Vol. 11, No. 5, May 1968, pp. 1092–1100.
[18] deBoer, P. C. T., "Probe for Measuring Ion Density in Slightly Ionized High Speed Flow," *The Review of Scientific Instruments*, Vol. 37, No. 6, June 1966, pp. 775–785.
[19] Bradley, J. N. and Robinson, P. A., "Studies in Expanded Shock Tube Flows. I. Probe Studies of the Expansion Process," *Proceedings of the Royal Society of London*, Vol. 301, No. 1466, Oct. 1967, pp. 285–302.
[20] deBoer, P. C. T. and Johnson, R. A., "Theory of Flat-Plate Ion-Density Probe," *The Physics of Fluids*, Vol. 11, No. 4, April 1968, pp. 909–911.
[21] deBoer, P. C. T., "Ion Boundary Layer on Flat Plate," to be published.
[22] Dukowicz, J., "Theory of Convection-Conduction Dominated Electrostatic Probes: Numerical Solution of the Two-Dimensional Flat Plate Problem," RA-2641-Y-1, 1969, Cornell Aeronautical Lab., Buffalo, N.Y.
[23] Kulgein, N. G., "Ion Collection from Low-Speed Ionized Gas," *AIAA Journal*, Vol. 6, No. 1, Jan. 1968, pp. 151–152.
[24] deBoer, P. C. T. and David, T. S., "Spherical and Cylindrical Ion Probes in Flowing Continuum Plasmas," *Bulletin of the American Physical Society*, Vol. 15, No. 11, Nov. 1970, p. 1558; also David, T. S., "Spherical and Cylindrical Electric Probes in a Continuum Flowing Plasma," Ph.D. thesis, 1971, Cornell Univ., Ithaca, N.Y.
[25] Loeb, L. B., *Basic Processes of Gaseous Electronics*, University of California Press, Berkeley, Calif. 1960.
[26] von Kármán, T. and Tsien, H. S., "Boundary Layer in Compressible Fluids," *Journal of the Aeronautical Sciences*, Vol. 5, 1938, pp. 227–232.
[27] Pohlhausen, K., "Zur Näherungsweisen Integration der Differentialgleichung der Laminaren Reibungsschicht," *Zeitschrift für Angewandte Mathematik und Physik*, Vol. 1, 1921, pp. 252–268.
[28] deBoer, P. C. T., Johnson, R. A., and Grimwood, P. R., "Electric Ion-Collecting Probes Governed by Convection and Production," *Proceedings of the VIIth International Shock Tube Symposium*, University of Toronto Press, 1970, pp. 795–819.
[29] Johnson, R. A., "Theory of Flat-Plate and Cylindrical Ion-Density Probes," Ph.D. thesis, 1969, Cornell Univ., Ithaca, N.Y.
[30] Langmuir, I. and Blodgett, K. B., "Currents Limited by Space Charge between Coaxial Cylinders," *Physical Review*, Vol. 22, No. 4, Oct. 1923, pp. 347–356.
[31] Langmuir, I. and Mott-Smith, H. M., "Studies of Electrical Discharges in Gases at Low Pressures," *General Electric Review*, Vol. 27, 1924, pp. 449–455, 538–548, 616–623, 762–771, 810–820.
[32] Schulz, G. J. and Brown, S. C., "Microwave Study of Positive Ion Collection by Probes," *Physical Review*, Vol. 98, No. 6, June 1955, pp. 1642–1649.
[33] Laframboise, J. G., "Theory of Spherical and Cylindrical Langmuir Probes in a Collisionless, Maxwellian Plasma at Rest," UTIAS Rept. 100, 1966, Univ. of Toronto, Toronto, Ontario.

MAY 1972 AIAA JOURNAL VOL. 10, NO. 5

Measurement of Nitrogen Plasma Transport Properties

PAUL W. SCHREIBER* AND ALLEN M. HUNTER II†
Aerospace Research Laboratories, Air Force Systems Command, Wright-Patterson Air Force Base, Ohio
AND
KENNETH R. BENEDETTO‡
Systems Research Laboratory Inc., Dayton, Ohio

The electrical and thermal conductivities and radiant power per unit volume, P_R, of nitrogen are measured at atmospheric pressure between 10,500 and 12,250°K and are compared with the results of other investigators. A probe technique based on the Hall effect is used to determine the plasma electrical conductivity and P_R. In addition, P_R is determined by external optical techniques. A separate measurement technique which is used to determine the vacuum ultraviolet contribution to P_R is described. A correction for self-absorption is applied to the probe measurements of P_R. Thermal conductivity is obtained from an energy balance of the power input and measured loss terms.

Introduction

THE electrical and thermal conductivities and the radiant power per unit volume of nitrogen are measured at atmospheric pressure between 9000 and 12,250°K, and these data are compared with the results of other investigators. This investigation was initiated because a review of published data indicated that serious discrepancies exist in transport properties. These differences may be caused by: 1) errors in temperature measurements; 2) absorption of radiant energy by the plasma or external optical medium; 3) nonconstant spectral response of the detectors; 4) plasma impurities; 5) deviations from local thermodynamic equilibrium; and 6) assumptions used in obtaining and reducing the data.

In this investigation the radiant power per unit volume is measured by two independent methods, and the results are correlated with the measured temperature. Any discrepancy between these source strength measurements is therefore not attributable to an error in the temperature measurement, thus allowing other possible errors to be more easily evaluated. A probe technique based on the Hall-effect is used to determine the plasma electrical conductivity σ and also the radiant power per unit volume P_R. P_R is also determined by external optical methods which include a separate measurement technique to determine the vacuum ultraviolet contribution to the radiant power per unit volume. A correction for self-absorption at wavelengths greater than 2000 Å is applied to the probe measurements of P_R. Thermal conductivity is obtained from a balance of the measured power input and loss terms.

Presented as Paper 71-590 at the AIAA 4th Fluid and Plasma Dynamics Conference, Palo Alto, Calif., June 21–23, 1971; submitted July 9, 1971; revision received December 20, 1971.
Index categories: Atomic, Molecular, and Plasma Properties; Heat Conduction; Radiation and Radiative Heat Transfer.
* Research Scientist, Thermomechanics Research Lab. Member AIAA.
† Research Scientist, Thermomechanics Research Lab.
‡ Visiting Research Associate.